Chapter 4

Wave Propagation in Elastic Medium

Buddhism statue at Longmen (龍門) in Luoyang (洛陽), China.

This was a place where rich people in the capital city of Luoyang donated statues for dead people. Descriptions on the life of the dead people were carved on rock and have been considered as the best calligraphy .

4.1 Earthquake Waves: S Wave

S wave (Secondary wave) is a propagation of shear deformation that arrives at earthquake observation stations after (second to) the Primary body wave (P wave, see Sect. 4.2). Since S wave generates a significant magnitude of horizontal motion at the ground surface, it is considered to be the most important cause of seismic damage.

Figure 4.1 illustrates the derivation of S-wave propagation equation for which a study is made of equation of motion of a small soil element in an semi-infinite level and elastic ground

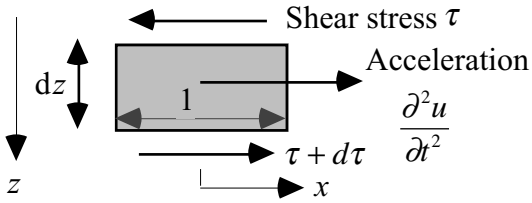

Fig. 4.1 Derivation of S-wave propagation equation

$$\rho \frac{\partial^2 u}{\partial t^2} = \frac{\partial \tau}{\partial z}, \qquad (4.1)$$

where u is the horizontal displacement, and ρ stands for the mass density of soil (1.5–2 times that of water in most situations), while τ is the shear stress in a horizontal plane at the top and bottom of the concerned soil element. Lateral normal stresses on the left and right sides of the element are not included in the equation. This is because the assumption of a homogeneous level ground subjected to horizontal shaking makes everything constant in the x direction and, consequently, the normal stresses on two sides are equal to and cancel each other.

Another assumption of linear elasticity correlates shear stress with shear strain and displacement

$$\tau = G \times (\text{shear strain}) = G \frac{\partial u}{\partial z}, \qquad (4.2)$$

in which shear modulus of soil is designated by G. By substituting (4.2) in (4.1) and using a new notation of $V_s = \sqrt{G/\rho}$,

$$\frac{\partial^2 u}{\partial t^2} = \frac{G}{\rho} \frac{\partial^2 u}{\partial z^2} = V_s^2 \frac{\partial^2 u}{\partial z^2}. \qquad (4.3)$$

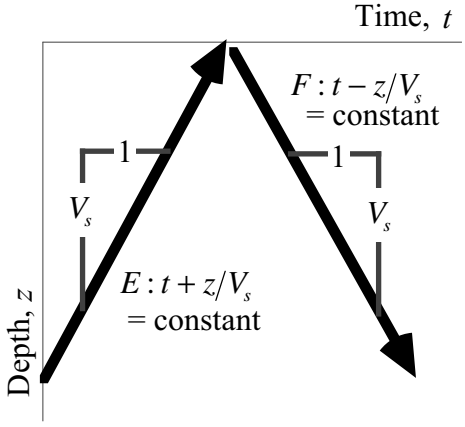

Fig. 4.2 Rate of wave propagation

The general solution of (4.3) is given by

$$u(t,z) = E(t + z/V_s) + F(t - z/V_s), \qquad (4.4)$$

in which E and F are arbitrary functions of $t+z/V_s$ and $t–z/V_s$, respectively. They have to be arbitrary because the time history of earthquake motions are irregular.

Figure 4.2 shows that the motions represented by E and F travel upwards or downwards at the rate of V_s per second. For example, suppose that $E = 1.2345$ when $t+z/V_s = 2.00$. There are many combinations of t and z for which $t+z/V_s = 2.00$. The only requirement for $E = 1.2345$ is that z decreases by V_s when t increases by 1. Thus, the phenomenon of $E = 1.2345$ moves upwards at the rate of V_s per second. Accordingly the horizontal shaking accounted for by E function travels upwards at the speed of V_s. Similarly, the F component of shaking propagates downwards at the rate of V_s. Hence, V_s is called the S-wave propagation velocity.

Thus, the horizontal shaking was decomposed into two parts: upward and downward propagations. Propagating inside a solid medium, S wave is one of what are called body waves. Typical V_s values are, approximately, 100 m/s for very soft soils, 300 m/s for stiff soils, and 3,000 m/s for hard intact rocks.

4.2 Earthquake Waves : P Wave

In addition to the S wave in Sect. 4.1, another kind of body wave that propagates in a homogeneous medium is called the P wave. P wave is a propagation of compression and extension (variation of pressure and volume change). Typical example of P wave is a propagation of sound, see Fig. 4.3.

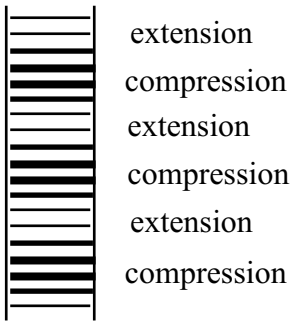

Fig. 4.3 Propagation of volume change in P wave propagation

The rate of P wave propagation is given by

$$V_{\mathrm{p}} = \sqrt{\frac{E(1-\nu)}{\rho(1-2\nu)(1+\nu)}}, \qquad (4.5)$$

where E is the modulus of elasticity and ν the Poisson ratio. Note that the Poisson ratio is equal to 0.5 in an incompressible material and makes V_{p} infinite.

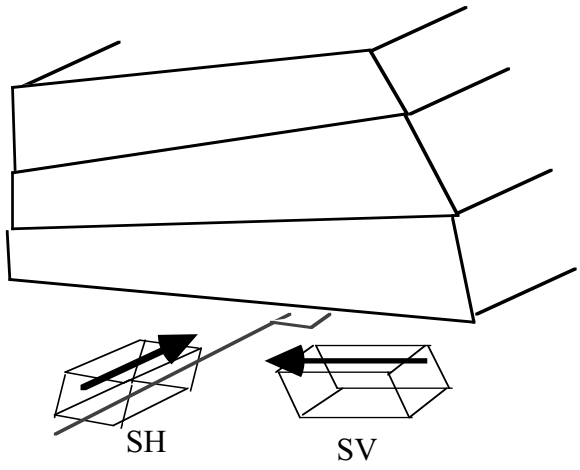

Fig. 4.4 Difference of SH and SV waves

It is a common practice in geophysical exploration that P wave is generated artificially by any impact or explosion so that its rate of propagation, V_{p}, may be measured. The obtained V_{p} value is substituted in (4.5) to back-calculate the value of E while the Poisson ratio is assumed to be more or less 0.25–0.3. It is noteworthy that this technique of subsurface exploration is useful for very stiff soil and rock. When this technology is conducted in soft soil of an alluvial plane where the ground water table is high, the measured V_{p} is often 1,400–1,500 m/s. Since the pore of soil is saturated with water and the modulus of compressibility of water is greater than that of soft soil skeleton, the measured V_{p} is the velocity of sound propagation in water without much correlation with the engineering nature of soil. In contrast, the P wave velocity, V_{p}, is, for example, 5,000 m/s in an intact rock mass.

There is an interaction between P and S waves. Figure 4.4 illustrates two kinds of S waves. For SH, the direction of soil particle motion is antiplane and perpendicular to the cross section of subsoil, while SV moves soil particles inside the plane. After SH wave arrives at the boundary of two different soils, the motion is still SH, although the direction of wave propagation may change (refraction 屈折 into the next layer and reflection 反射 back into the first layer) in accordance with the nature of soil (Fig. 4.5a). On the contrary, SV wave upon arrival at a boundary generates both P and SV waves in refracted and reflected phases as well (Fig. 4.5b). Because of the simplicity, most seismic risk analyses of regions and municipalities assume SH waves assuming horizontally layered ground. On the contrary, dynamic response analyses on important structures (foundations, dams, etc.) are conducted on two-dimensional cross sections and hence work on SV (not SH) waves.

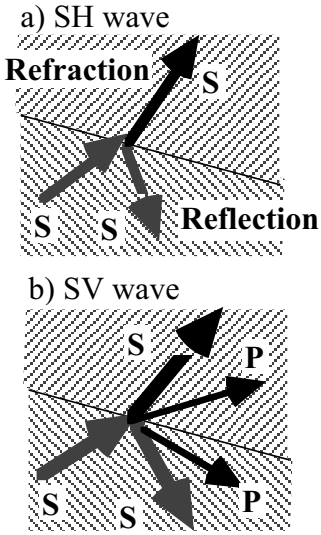

Fig. 4.5 Refraction and reflection of S waves at interface

An earthquake source generates both P and S waves simultaneously. At a focal distance of L, they arrive at different times because of different propagation velocities. The difference in arrival time is given by

$$\Delta T = \frac{L}{V_s} - \frac{L}{V_p}. \qquad (4.6)$$

This formula is used to assess the distance to the seismic source, L, by using the recorded time difference, ΔT. For wave propagation in earth crust, V_p and V_s in intact rock mass are relevant, $V_p = 5$ km/s and $V_s = 3$ km/s. If L from three observation points are known, it is possible to determine the location of the wave source.

Hard rock has V_p of typically 5,000 m/s. In soft water-saturated soil, P wave propagation in pore water is predominant. Hence, V_p in such a soil condition is similar to the velocity of sound in water. For example, the sound velocity in water is 1,483 m/s at 20 °C and 1,433 m/s at 15 °C. The sound velocity in air is 343.5 m/s at 20 °C.

4.3 Idealization of Vertical Wave Propagation

It is common that a (design) earthquake occurs at a distance of tens or hundreds of kilometers awayfrom the site of concern while the depth of fault rupture is again tens of kilometers. Hence, the source of earthquake wave propagation is not below the site to be studied, see Fig. 4.6. Therefore, the idea of vertical wave propagation as discussed in Sect. 4.1 appears to be inappropriate.

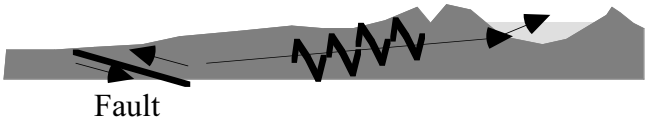

Fig. 4.6 Geometrical relationship between earthquake source and site of interest

Actually, the direction of wave propagation in an alluvial soft deposit should be studied in a more detailed scale (Fig. 4.7). For instance, the propagation velocity of S wave (V_s) is a function of shear rigidity, G

$$V_s = \sqrt{G/\rho}\,. \qquad (4.7)$$

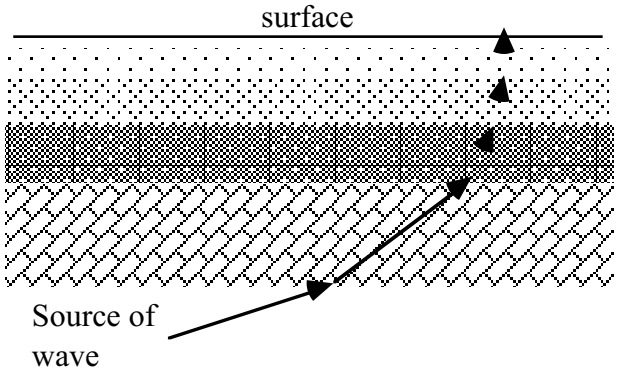

Fig. 4.7 Wave path in alluvium

Since G of geomaterials is smaller at shallower depth, V_s decreases as well towards the ground surface. Hence, Snell's law of wave refraction at an interface of two different wave velocities states that the wave propagation should change its direction to be more vertical, in general, as the ground surface is approached.

From Snell's law in Fig. 4.8, using a proportionality parameter of α,

$$\sin i = \frac{\mathrm{d}x}{\sqrt{\mathrm{d}x^2 + \mathrm{d}z^2}} = \alpha \times V_s \le 1 \quad \text{or}$$

$$\frac{\mathrm{d}x}{\mathrm{d}z} = \frac{\alpha^2 V_s^2}{1 - \alpha^2 V_s^2}. \qquad (4.8)$$

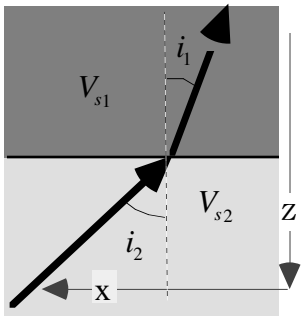

Fig. 4.8 Snell's law of wave refraction at interface

By assuming $\alpha^2 V_s^2 = \alpha^2 G/\rho = z^n$ in which n accounts for the effects of depth (or effective stress) on G,

$$\frac{\mathrm{d}x}{\mathrm{d}z} = \frac{z^n}{1 - z^n} = -1 + \frac{1}{1 - z^n}. \qquad (4.9)$$

Figure 4.9 illustrates the integration of (4.9) that governs the change of direction of wave propagation. "n = 1" was employed only for easy calculation; $n < 1$ is more likely in reality. Note that Fig. 4.9 assumes a continuous variation of V_s with depth, while V_s in reality changes discontinuously at interfaces of materials of different geological ages. One of the important discontinuity occurs between alluvial and pleistocene deposits.

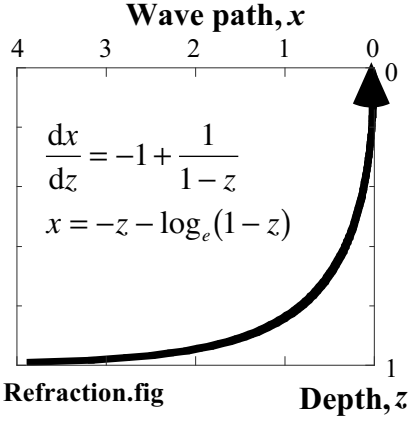

Fig. 4.9 Example calculation of change of wave propagation direction due to continuous variation of G with depth

4.4 Vertical Propagation of "S" Wave in Level Ground

The most important type of earthquake shaking is conventionally, and most probably in future as well, the S wave that produces a ground motion in the horizontal direction. This direction of motion is substantially efficient in causing damage to surface structures.

As was already shown in Fig. 4.9, it is reasonable at a shallow depth to assume a vertical propagation of S wave. See Fig. 4.10 in this Section.

In what follows, the horizontal displacement of a soil grain is denoted by u. The equation of wave propagation is given by

$$\frac{\partial^2 u}{\partial t^2} = V_s^2 \frac{\partial^2 u}{\partial z^2}, \qquad (4.10)$$

in which $V_s = \sqrt{G/\rho}$.

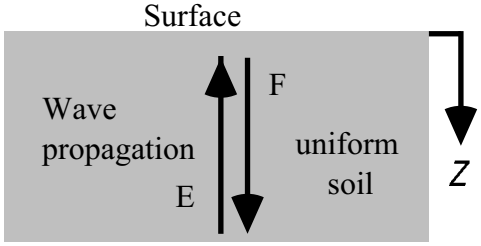

Fig. 4.10 Vertical propagation of S wave in level subsoil

A harmonic solution (sinusoidal solution) of (4.10) is derived by assuming that u varies with time in accordance with $\sin(\omega t)$ and $\cos(\omega t)$ functions. The symbol of ω denotes a circular frequency of shaking (円振動数), which is equivalent with a frequency of $\omega/2\pi$. It is, however, more efficient to use in this section a complex exponential function,

$$u(z,t) = A(z)\ \exp(\mathrm{i}\omega t), \qquad (4.11)$$

where $i = \sqrt{-1}$ and A is an unknown function of z. In case this complex expression is not easy, it is acceptable for a reader to go to Sect. 4.5. In that section, it will be demonstrated that expressions in terms of complex number and real number are equivalent but that the complex number can save time. Note that the real and complex parts of the exponential function in (4.11) are cos and sin functions,

$$\exp(i\omega t) = \cos(\omega t) + i\ \sin(\omega t), \qquad (4.12)$$

By substituting (4.11) in (4.10),

$$\frac{\mathrm{d}^2 A}{\mathrm{d}z^2} = -\left(\frac{\omega}{V_s}\right)^2 A \quad \text{and, accordingly,} \quad A = E\ \exp\left(\frac{\mathrm{i}\omega z}{V_s}\right) + F\ \exp\left(-\frac{\mathrm{i}\omega z}{V_s}\right), \qquad (4.13)$$

where E and F are constant parameters that are determined by boundary conditions. The solution for "u" is finally derived as

$$u(z,t) = \left\{A = E\ \exp\left(\frac{\mathrm{i}\omega z}{V_s}\right) + F\ \exp\left(-\frac{\mathrm{i}\omega z}{V_s}\right)\right\}\exp(\mathrm{i}\omega t) = E\ \exp\left\{\mathrm{i}\omega\left(t + \frac{z}{V_s}\right)\right\} + F\ \exp\left\{\mathrm{i}\omega\left(t - \frac{z}{V_s}\right)\right\}. \qquad (4.14)$$

The E and F terms in (4.14) stand for an upward and downward wave propagations, respectively. See Fig. 4.10. Equation (4.14) states that "u" varies with $\exp(\mathrm{i}\omega t)$ in terms of time. Hence, when ωt increases by 2π, the value of "u" comes back to the original value. Hence, $2\pi/\omega$ is the period of shaking. Similarly, "u" varies with $\exp(\mathrm{i}\omega z/V_s)$ in terms of depth, and $2\pi V_s/\omega$ stands for the wave length. Further, ω/V_s is sometimes called the wave number. A further study will continue in Sect. 6.7.

Although a harmonic motion is not a reality, it is still very important in practice. This is because the real irregular ground motion can be divided into harmonic components of various frequencies, Fourier series (Sect. 9.11). Each component has a different intensity and it is further amplified to a different extent in the surface alluvium. This is called the local soil effect.

4.5 Solution of S-Wave Propagation in Real Numbers

The equation of S-wave propagation is given by

$$\frac{\partial^2 u}{\partial t^2} = V_s^2 \frac{\partial^2 u}{\partial z^2}. \qquad (4.15)$$

By assuming its harmonic solution with real numbers,

$$u(z,t) = A(z)\sin(\omega t). \qquad (4.16)$$

By substituting (4.16) in (4.15),

$$-\omega^2 A \sin\omega t = V_s^2 \frac{\mathrm{d}^2 A}{\mathrm{d}z^2}\sin\omega t. \qquad (4.17)$$

Consequently,

$$\frac{\mathrm{d}^2 A}{\mathrm{d}z^2} = -\left(\frac{\omega}{V_s}\right)^2 A \qquad (4.18)$$

whose solution is given by

$$A = A_1 \sin\frac{\omega z}{V_s} + A_2 \cos\frac{\omega z}{V_s}, \qquad (4.19)$$

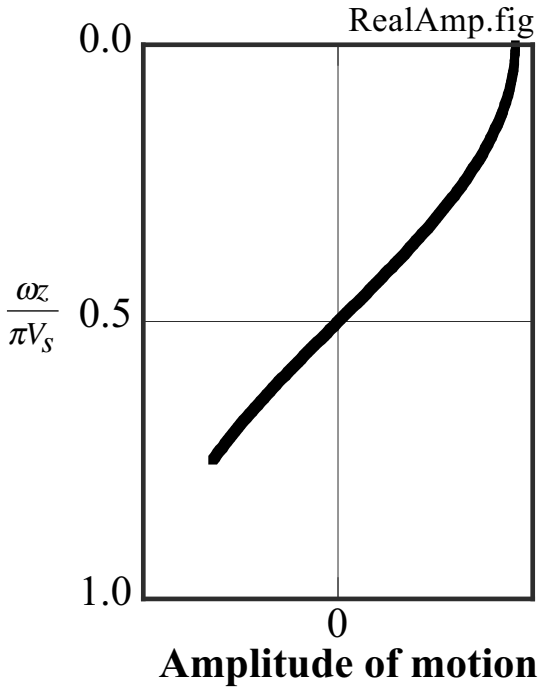

Fig. 4.11 Variation of shaking amplitude in vertical direction

in which A_1 and A_2 are constant parameters to be determined by boundary conditions. Accordingly,

$$u(z,t) = \frac{A_1}{2}\left[-\cos\left\{\omega\left(\frac{z}{V_s}+t\right)\right\} + \cos\left\{\omega\left(\frac{z}{V_s}-t\right)\right\}\right] + \frac{A_2}{2}\left[\sin\left\{\omega\left(\frac{z}{V_s}+t\right)\right\} - \sin\left\{\omega\left(\frac{z}{V_s}-t\right)\right\}\right]. \qquad (4.20)$$

Note thus that this solution consists of the upward $\left(\frac{z}{V_s}+t\right)$ and downward $\left(\frac{z}{V_s}-t\right)$ propagations of motion.

Since the ground surface is an interface of soil with air or water in which shear stress is zero, the boundary condition at the ground surface ($z = 0$) specifies

$$\tau = G \times (\text{shear strain}) = G\frac{\partial u}{\partial z} = 0 \text{ or } \quad \frac{\partial u}{\partial z} = 0 \text{ and } \frac{\mathrm{d}A}{\mathrm{d}z} = 0. \qquad (4.21)$$

Accordingly, $A_1 = 0$

$$A(z) = A_2 \cos\frac{\omega z}{V_s} \qquad \text{and} \qquad u(z,t) = A_2 \cos\frac{\omega z}{V_s}\sin\omega t. \qquad (4.22)$$

Figure 4.11 illustrates the variation of the amplitude of motion, $A(z)$, in the vertical direction. Note that the sign of "A" changes below $\omega z/V_s = \pi/2$. This implies that the ground surface and soil below some depth move in opposite directions. It is interesting that there is a special depth at which the amplitude is zero.

The simplest type of amplification of motion is defined by the ratio of motion at the surface and at the base (base stiff soil or rock) at $z = H$;

$$\mathrm{Amp}(E+F) \equiv \frac{\text{Amplitude of motion at surface}}{\text{Amplitude of motion at base}} = \frac{|A(z=0)|}{|A(z=H)|} = \frac{1}{\left|\cos\dfrac{\omega H}{V_s}\right|}. \tag{4.23}$$

Figure 4.12 demonstrates the variation of amplification with $\omega H/V_s$. The amplification thus varies with the frequency of motion (frequency = $\omega/2\pi$) and the thickness of surface soil (H). The maximum value of amplification (resonance) occurs when $\omega H/V_s = \left(n-\dfrac{1}{2}\right)\times\pi$ in which n=1,2,3,$\cdots$. When n = 1/2 in particular,

$$\omega H/V_s = \frac{\pi}{2},\ \ \omega = \frac{\pi V_s}{2H},\ \text{frequency} = \frac{\omega}{2\pi} = \frac{V_s}{4H},\ \text{and}$$
$$\text{the period of motion} = \frac{1}{\text{frequency}} = \frac{4H_s}{V_s}, \tag{4.24}$$

which is very important in seismic microzonation. The amplification means that the surface motion is Amp(E+F) times greater than the motion at the base.

Although Fig. 4.12 suggests an infinite value of amplification at resonance, the reality does not cause infinite intensity of surface motion upon (small) motion at the base. Real soil and ground have many kinds of energy loss and does not enable such a strong motion; see Sect. 9.6 and Chap 10.

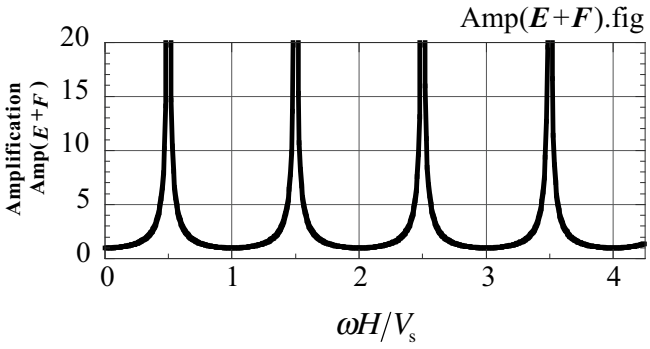

Fig. 4.12 Amplification of motion in ideally linearly elastic ground

4.6 Exercise No. 1 on Amplification of Ground Motion

1. Take the real parts of (4.14) in Sect. 4.4. Determine the relationship between two unknown parameters, E and F, by using a boundary condition at the ground surface. Do not forget that "E" and "F" are complex numbers.
   Boundary condition: Since the ground surface (z=0) is a free surface, there is no shear stress, $G\frac{\partial u}{\partial z} = 0$. Since $G \neq 0$, $\frac{\partial u}{\partial z} = 0$.
2. Remove "F" from concerned formulae by using the relationship derived in [1]. Then, plot the relationship between the amplitude of shaking displacement "u" and the depth. Use high and low values of frequency (high and low values of ω).
3. Calculate the amplification factor which is the ratio of the amplitudes of shaking motion "u" at the surface and at the bottom of the surface soil ($z = H$).
4. Calculate the amplification similarly for a situation where there is a rigid mass of "M" per unit area at the ground surface.

For answers, see the end of this book.

4.7 Earthquake Waves : Rayleigh Wave

The Rayleigh wave travels along the ground surface (surface wave). It does not propagate into the earth. The displacements, u and w in Fig. 4.13, are analytically given in complex numbers

$$u = \mathrm{i}AN\left[-\exp\left\{-\frac{q}{N}(zN)\right\} + \frac{2\frac{q}{N}\frac{s}{N}}{\frac{s^2}{N^2}+1}\exp\left\{-\frac{s}{N}(zN)\right\}\right]\exp\{\mathrm{i}(\omega t)Nx\}$$

$$w = \mathrm{i}AN\left[\frac{2\frac{q}{N}}{\frac{s^2}{N^2}+1}\exp\left\{-\frac{s}{N}(zN)\right\} - \frac{q}{N}\exp\left\{-\frac{q}{N}(zN)\right\}\right]\exp\{\mathrm{i}(\omega t)Nx\},$$

in which $\mathrm{i} = \sqrt{-1}$, A is constant, N the wave number with the wave length = 2π/N, and ω the circular frequency. Moreover,

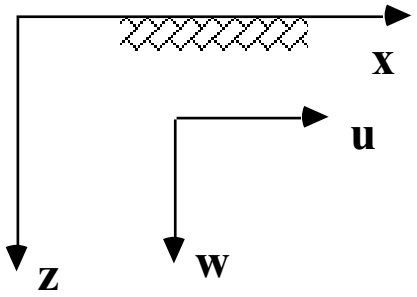

Fig. 4.13 Positive direction of coordinates and displacements

$$q = \sqrt{N^2 - \omega^2/V_{\mathrm{p}}^2} \quad \text{and} \quad s = \sqrt{N^2 - \omega^2/V_{\mathrm{s}}^2}$$

The wave number, N, is calculated by $N = \omega/V_{\mathrm{s}}K$ in which K is a solution of

$$K^6 - 8K^4 + \left(24 - 8\frac{1-2\nu}{1-\nu}\right)K^2 - \frac{8}{1-\nu} = 0$$

and is given as

Poisson ratio ν	0.0	0.1	0.2	0.3	0.333	0.4	0.5
$K = V_{\mathrm{r}} / V_{\mathrm{s}}$	0.874	0.893	0.911	0.927	0.933	0.942	0.955

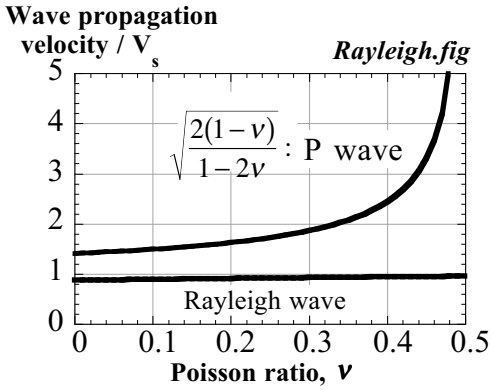

Fig. 4.14 Wave propagation velocities

The velocity of Rayleigh wave, V_r, is slightly smaller than V_s, see Fig. 4.14. Figure 4.15 illustrates the orbit of particle movement near the surface (z=0). When the wave propagates towards the right, the particle rotates in a counterclockwise direction. Bolt (1993) drew a good illustration of the material movement in Rayleigh wave. The direction of the particle movement is reversed below some depth to be clockwise.

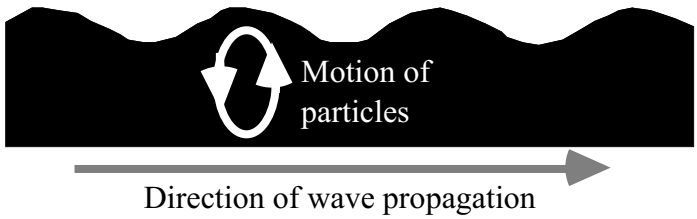

Fig. 4.15 Form of Rayleigh-wave motion in elastic medium

When the subsoil is composed of soil layers that have different shear wave velocities (V_s), the propagation velocity of Rayleigh wave is variable. Rayleigh wave of longer wave length (long period) is affected by nature of soils at greater depth where V_s is higher, and its propagation velocity is greater. On the contrary, Rayleigh wave of shorter wave length (high frequency) is controlled by soils at shallower elevation, and its propagation velocity is slower. This nature is applied to subsurface soil investigation in which the propagation velocity of many Rayleigh-wave components are measured and shear modulus of soils at corresponding depth is determined.

Seismologists are interested in Rayleigh wave traveling along the earth′s perimeter. However, that wave causes a very small intensity of ground shaking without affecting engineering facilities. Earthquake geotechnical engineering is interested in Rayleigh waves that are generated when the incident P and S waves hit the surface irregularity and are reflected. A surface wave seems to decay quickly as it travels along the surface of soft deposits. It cannot reach a far distance. This is because the soft soil has a hysteresis stress–strain loop and the wave energy decays quickly during the propagation.

Application of Rayleigh wave to site investigation: Artificially generate Rayleigh wave (Sect. 4.9) and measure its propagation velocity V_r, at surface. Since $V_r \cong V_s = \sqrt{G/\rho}$, "$G$" of soil is obtained. "$\rho$" is typically 1.8–2.0 ton/m^3.

4.8 Earthquake Waves : Love Wave

There is another type of surface wave that is called Love wave. This wave occurs when an elastic halfspace is overlain by a softer surface layer (Fig. 4.16). Harmonic solution (sinusoidal function) is given by

$$u_1 = \left\{A\ \exp(\mathrm{i}s_1 z) + B\ \exp(-\mathrm{i}s_1 z)\right\}\exp(-\mathrm{i}qy)\exp(\mathrm{i}\omega t)$$
$$u_2 = C\ \exp(-\mathrm{i}s_2 z)\exp(-\mathrm{i}qy)\exp(\mathrm{i}\omega t),$$

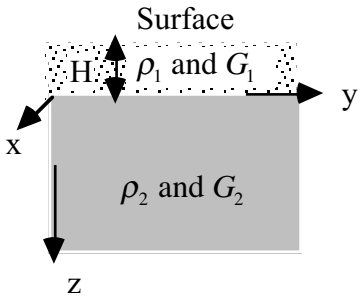

Fig. 4.16 Coordinates in Love-wave theory

where u_1 and u_1 stand for displacement in x direction in the upper and lower layers, respectively. A, B, and C are constants. Furthermore, ω is the circular frequency, and

$$s_1 = \sqrt{k_1^{\,2} - q^2},\ \ k_1 = \omega / V_{\mathrm{s1}},\ \ V_{\mathrm{s1}} = \sqrt{G_1/\rho}$$
$$s_2 = \sqrt{k_2^{\,2} - q^2},\ k_2 = \omega / V_{\mathrm{s2}},\ V_{\mathrm{s2}} = \sqrt{G_2/\rho}$$

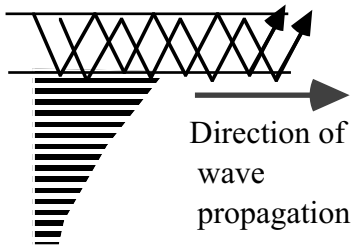

Fig. 4.17 Superimposed SH wave propagation

Since the particle motion is oriented in the x direction, Love wave is a type of SH wave. The above solution means that an upward and downward propagation of SH waves are superimposed (重複) in the upper layer; both propagating in y direction as well, whilst the lower layer has a horizontal propagation of a single SH wave (Fig. 4.17).

Figure 4.18 illustrates a view of ground deformation. The surface layer is sheared in both y and z directions. Bolt (1993) made a good illustration of particle movement in Love wave. Being SH wave, Love wave does not have a volume change.

A, B, and C parameters are determined by considering (1) shear stress = 0 at the ground surface (z=–H), and (2) both stress and displacement are continuous at the interface (z=0). The velocity of Love wave velocity, V_{L}, is given by

$$V_{\mathrm{L}} = q/a = V_{\mathrm{s1}}\sqrt{1 + s_1^{\,2}/q^2}\ .$$

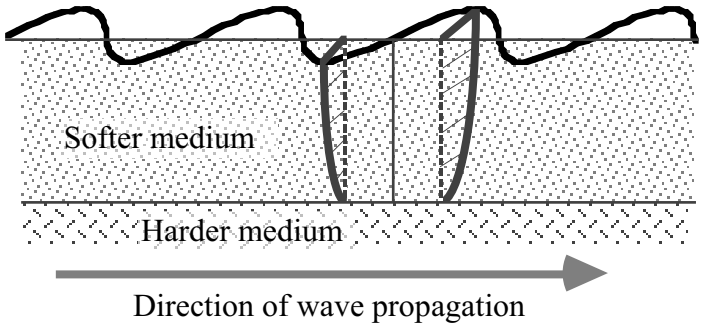

Fig. 4.18 Conceptual view of ground deformation in Love wave

When the wave length seen along the surface, L=2p/q, varies, q value changes as well and V_{L} changes

High frequency $\rightarrow$short L $\rightarrow$ V_{L} approaches V_{s1} and Low frequency $\rightarrow$long L $\rightarrow$ V_{L} approaches V_{s2}.

Thus, the wave propagation velocity of Love wave depends on the frequency. This fact makes dispersion and group velocity (U, 群速度). Vibration of different frequency propagates at different U. The principle lying behind this is similar to beeping (うなり).

$$\mathrm{d}(\omega t - qy)/\mathrm{d}q = 0 \qquad \therefore t(\mathrm{d}\omega/\mathrm{d}q) - y = 0 \qquad U = y/t = \mathrm{d}\omega/\mathrm{d}q = \mathrm{d}\left(V_{\mathrm{L}}q\right)/\mathrm{d}q$$
$$\therefore U = V_{\mathrm{L}} + q\left(\mathrm{d}V_{\mathrm{L}}/\mathrm{d}q\right) = V_{\mathrm{L}} - L\left(\mathrm{d}V_{\mathrm{L}}/\mathrm{d}L\right).$$

4.9 Response of Elastic Ground to Surface Excitation

Figure 4.19 illustrates an elastic halfspace that is excited by a linear vertical loading. Solving the ground response under this situation is called Lamb´s problem. For details, see Båth (1968).

The solution of Lamb´s problem shows that the ground response to this linear loading consists of three components:

P wave : decays with distance
S wave : decays with distance
Rayleigh wave : no decay

The first two are body waves and propagates into the infinite body of ground. Therefore, they become weaker (decay) as they travel farther. In contrast, the surface wave (Rayleigh wave) maintains its amplitude to the infinity, because it travels along the surface.

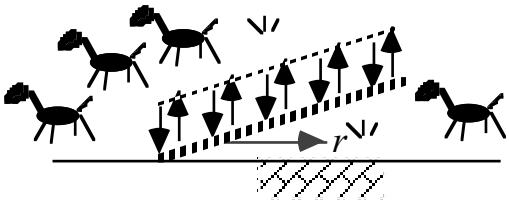

Fig. 4.19 Level ground excited by linear wave source at surface

When the surface loading is applied at a point (Fig. 4.20), all the three components of motion decay with distance. Table 4.1 reveals the rate of decay with the distance.

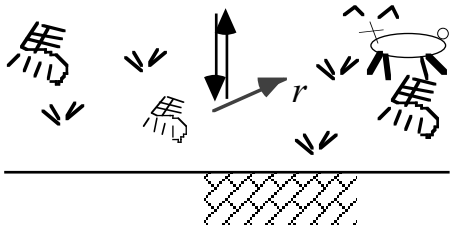

Fig. 4.20 Level ground excited by point wave source

Table 4.1 Decrease of wave amplitude at surface with distance from the source (geometrical damping)

Source	Rayleigh	P	S
Line	1	$r^{-3/2}$	$r^{-3/2}$
Point	$r^{-1/2}$	r^{-2}	r^{-2}

r: surface distance from source

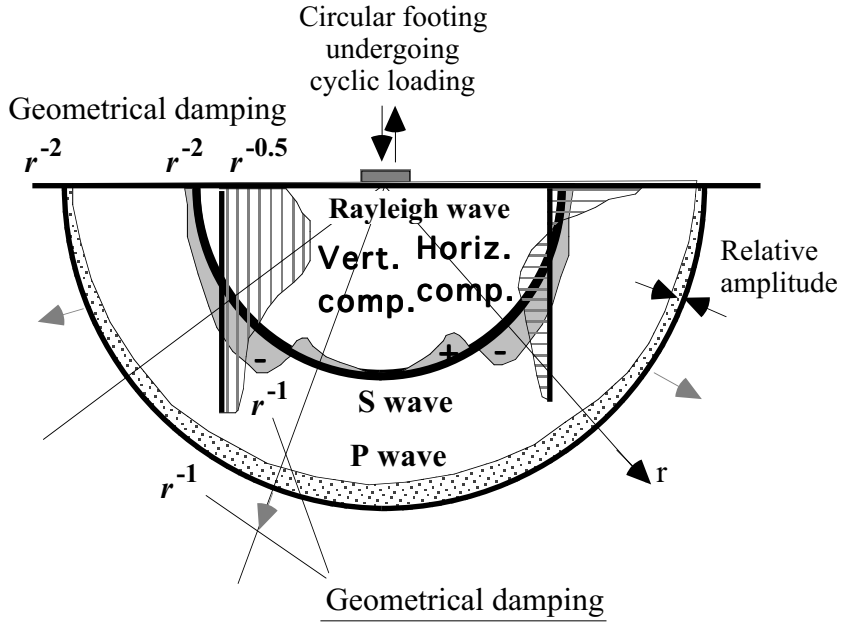

Shear window is the direction in which S-wave energy is concentrated.

Wave type	Percent of total energy
Rayleigh	67
Shear	26
Compression	7

Fig. 4.21 Distribution of displacement waves from a circular footing on a homogeneous, isotropic, elastic halfspace (after Woods, 1968)

Figure 4.21 indicates the variation of energy and wave type with the direction of propagation. Under a circular oscillating footing, similar to a point loading, the energy of P wave (compression wave) is more important in the vertical direction, S wave is important in the inclined directions, and Rayleigh wave is significant near the surface.

4.10 Wave Transmission and Reflection at Interface

Study is made of SH wave propagation across an interface of two elastic layers. An infinite medium is assumed here (Fig. 4.22), and attention is focussed on transmission and reflection at the interface. Being denoted as "*a*" and "b", those two layers are of different impedance. An incident wave (入射波 E_b) arrives from the bottom and, at the interface, are partially transmitted into the next layer (透過波 E_a), while partially reflected back (反射波 F_b). Note that discussion in this section assumes infinite thickness of the upper layer without surface.

The displacement, u, and shear stress, τ, under harmonic excitation are given by

$$u_a = E_a \exp\left\{i\omega\left(t + z/V_{sa}\right)\right\} \text{ and}$$

$$\tau_a = G_a \frac{\partial u_a}{\partial z} = i\omega\rho_a V_{sa} E_a \exp\left\{i\omega\left(t + z/V_{sa}\right)\right\} \text{ in layer "a"}$$

$$u_b = E_b \exp\left\{i\omega\left(t + z/V_{sb}\right)\right\} + F_b \exp\left\{i\omega\left(t - z/V_{sb}\right)\right\} \text{ and}$$

$$\tau_a = i\omega\rho_b V_{sb}\left[E_b \exp\left\{i\omega\left(t + z/V_{sb}\right)\right\} - F_b \exp\left\{i\omega\left(t - z/V_{sb}\right)\right\}\right] \text{ in layer "b".}$$

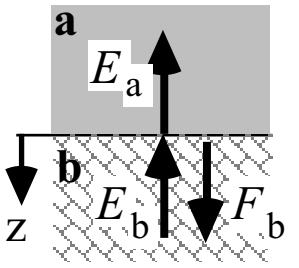

Fig. 4.22 Definition of incident and reflected waves near layer interface

Because of the continuity of displacement and shear stress at the interface (z=0),

$$\begin{cases} E_a = E_b + F_b \\ R \times E_a = E_b - F_b \end{cases} \text{ in which } R = \frac{\rho_a V_{sa}}{\rho_b V_{sb}} \text{ being the impedance ratio.}$$

The ratio of transmitted and reflected amplitudes over the incident amplitude are

$$\frac{E_a}{E_b} = \frac{2}{1+R} \text{ (transmitted) and}$$

$$\frac{F_b}{E_b} = \frac{1-R}{1+R} \text{ (reflected).}$$

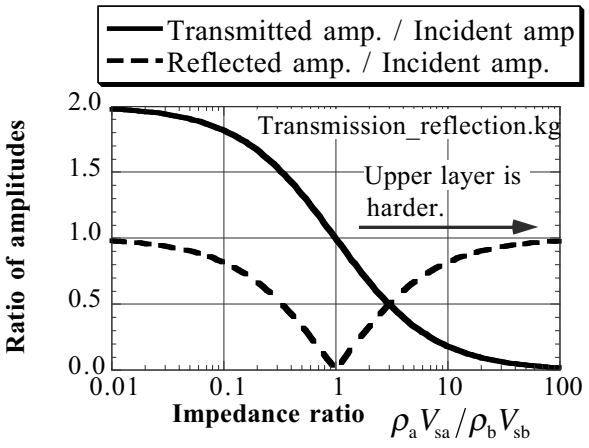

Fig. 4.23 Variation of wave amplitude at layer interface

The wave energy per one wave length is proportional to $\rho V_s E^2$ and $\rho V_s F^2$ (see Sect. 4.11). Therefore, the ratio of energy is derived in a similar way

$$\frac{\rho_a V_{sa} E_a^{\,2}}{\rho_b V_{sb} E_b^{\,2}} = \frac{4R}{(1+R)^2} \quad \text{and} \quad \frac{\rho_b V_{sb} F_b^{\,2}}{\rho_b V_{sb} E_b^{\,2}} = \left(\frac{1-R}{1+R}\right)^2.$$

These results are graphically demonstrated in Figs. 4.23 and 4.24. When the impedance ratio is 1, the material property is uniform and there is no wave reflection.

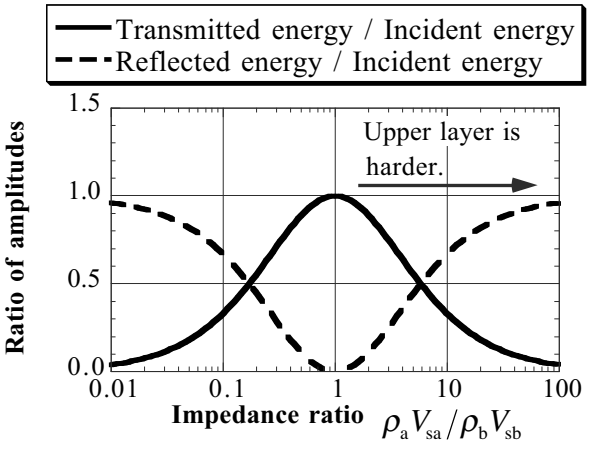

Fig. 4.24 Variation of wave energy at layer interface

4.11 Calculation of Seismic Wave Energy

Discussion here is made of S-wave propagation in the vertical direction. By assuming the displacement to be a cosine function of time, for example, displacement, velocity, and shear strain are derived

$$u = E\cos\left\{\omega\left(t+\frac{z}{V_s}\right)\right\},\quad \frac{\partial u}{\partial t} = -\omega E\sin\left\{\omega\left(t+\frac{z}{V_s}\right)\right\},\quad \frac{\partial u}{\partial z} = -\frac{\omega E}{V_s}\sin\left\{\omega\left(t+\frac{z}{V_s}\right)\right\}.$$

The wave energy per unit volume consists of kinetic and strain components

$$\frac{\rho}{2}\left(\frac{\partial u}{\partial t}\right)^2+\frac{G}{2}\left(\frac{\partial u}{\partial z}\right)^2=\frac{\omega^2E^2}{2}\left[\rho\sin^2\left\{\omega\left(t+\frac{z}{V_s}\right)\right\}+\frac{G}{V_s^{\,2}}\sin^2\left\{\omega\left(t+\frac{z}{V_s}\right)\right\}\right]$$

$$=\rho\omega^2E^2\sin^2\left\{\omega\left(t+\frac{z}{V_s}\right)\right\}=\frac{\rho\omega^2E^2}{2}\left[1-\cos\left\{2\omega\left(t+\frac{z}{V_s}\right)\right\}\right],$$

in which ρ stands for the mass density of soil. The wave energy in one wave length is derived by integrating this over the wave length $(=2\pi V_s/\omega)$;

$$\text{Energy per wave length}=\frac{\rho\omega^2E^2}{2}\times\frac{2\pi V_s}{\omega}=\omega\pi\left(\rho V_sE^2\right).$$

Thus, the energy per wave length is proportional to the impedance × amplitude^2. Consequently, the energy conservation requires that the wave amplitude should increase as V_s in the medium decreases (Fig. 4.25). The amplitude is inversely proportional to the square root of wave impedance. As the wave approaches the ground surface, V_s normally decreases and the amplitude increases (Sect. 3.1). Similar to amplification of sea waves near the shore, this is one of the mechanisms of earthquake wave amplification.

The wave energy that passes through any "z" section in one period is same as above.

$$\text{Energy per one period = (Energy per volume)}\times\frac{\mathrm{d}Z}{\mathrm{d}t}\times\text{period}=\frac{\rho\omega^2E^2}{2}\times\frac{2\pi V_s}{\omega}=\omega\pi\left(\rho V_sE^2\right)$$

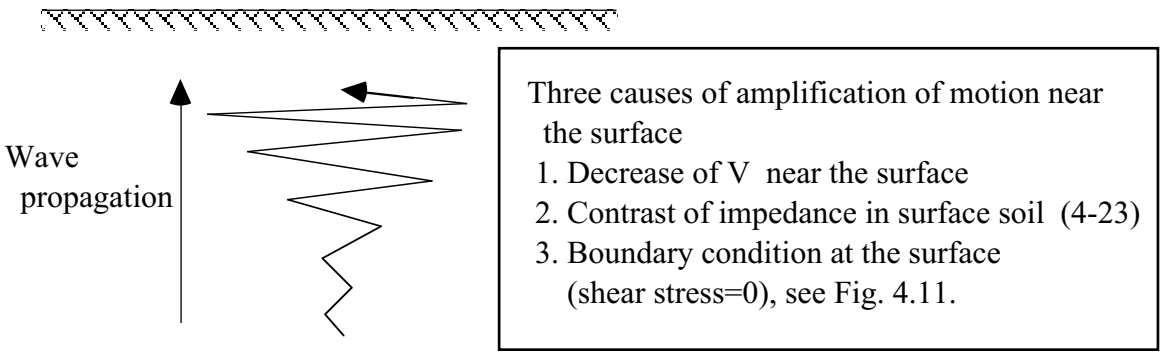

Fig. 4.25 Increase of wave amplitude with decreasing wave propagation velocity

4.12 Traffic-Induced Ground Vibration

Figure 4.21 illustrated that the major energy of Rayleigh surface wave travels in a shallow depth. Since Rayleigh wave is the major component of ground vibration caused by traffics and such construction works as pile driving, it seems adequate to install a wave insulator near the ground surface in order to mitigate this environmental noise problem.

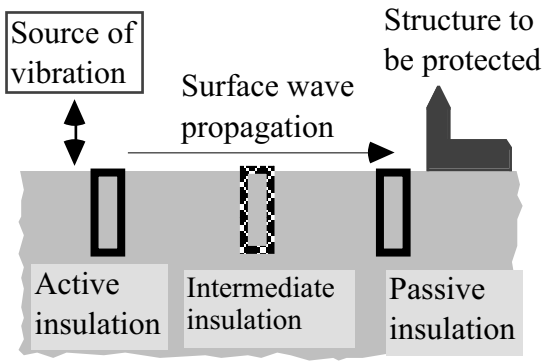

Fig. 4.26 Types of insulation against environmental ground vibration

As shown in Fig. 4.26, there are three types of mitigation. The active insulation is installed near the source of ground vibration and the cost is most probably borne by the operator or the owner of the source. On the other hand, the passive insulation is installed near the structure to be protected: paid either by the source side or by the affected party. Moreover, installation of insulation in the middle is possible. However, the land is not necessarily owned by either the source or the affected sides, and the installation is more difficult than the other two locations.

Section 4.10 discussed the energy reflection and transmission at an interface between hard and soft materials. It was shown in Fig. 4.24 that most wave energy is reflected backwards at an interface if the rigidity difference is significant. Therefore, two kinds of insulation are possible; being very rigid or very soft as compared with soil. The former is an embedded concrete wall, for example, and the latter is an open trench and embedding of other soft materials. For economical reasons, the latter appears to be more practical.

Haupt (1981) carried out model tests on an embedded rigid wall. Takemiya (2004) constructed a rigid honeycomb structure under road pavement in order to mitigate car-induced vibration.

Hayakawa et al. (1992) reduced the train-induced vibration by installing a mat under rails. The use of soft EPS can reduce the magnitude of vibration as well (Hayakawa et al. 1991). The use of gas cushion as a soft insulation was studied by De Cock and Legrand (1990) together with Massarsch (1991, 2004).

A design diagram was prepared by Woods (1968) for cut-off of surface wave propagation by a trench. The effects of a trench depend on the size of a trench and the wave length (frequency) of the concerned Rayleigh wave. The same diagram is valid for gas cushion because the same principle of cut-off is therein employed.

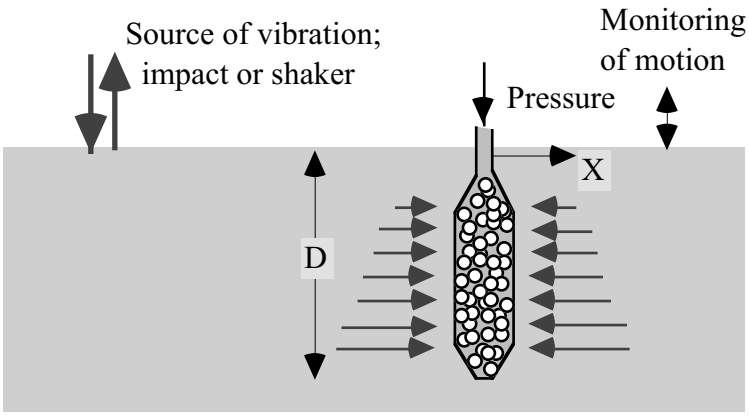

Fig. 4.27 Generation of surface wave for study of mitigation of ground vibration

The author´s group attempted to construct a similar diagram based on field tests. Ground vibration was caused either by a shaker or impact by hammer. The idea behind that study was as what follows:

– An open trench is good for mitigation of vibration, but requires a retaining structure to maintain stability. This additional structure may reduce the mitigative effects.
– Cushion, which is called air bag by the author, with internal pressure is better in this sense.
– The stability of an embedded air bag should be further improved by placing light EPS beads in a bag so that lateral resistance against earth pressure may be improved.

Figure 4.27 shows the geometry of test conditions. An air bag with EPS beads was embedded (Sannomiya et al. 1993) in order to demonstrate a relationship between wave length, horizontal distance between the point of measurement and the air bag (X), and the depth of the air bag (D). The wave length was determined by measuring the wave propagation velocity (V_r) and the shaking frequency (f);

$$\text{Wave length} = V_r / f.$$

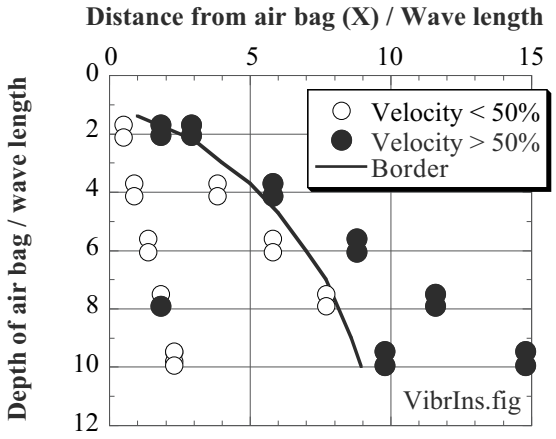

Fig. 4.28 Mitigative effects of embedded cushion under surface wave propagation (impact shaking)

The interpretation of the measured records considered that the air bag was effective when the intensity of vertical velocity was reduced to be less than 50%. Consequently, Fig. 4.28 was obtained. It is advised that the depth of an air bag is determined by referring to the curve in this figure. As the point of concern becomes further from the air bag (passive mitigation), a deeper air bag excavation is necessary.

List of References in Chapter 4

Båth, M. (1968) Mathematical Aspects of Seismology, Chap. 12, Elsevier, New York.

Bolt, B.A. (1993) Earthquakes and Geological Discovery, Scientific American Library, ISBN 0-7167-5040-6, p. 39.

De Cock, F. and Legrand, C. (1990) Ground vibration isolation using gas cushions, Proc. Int. Conf. Geotextiles, Geomembranes, and Related Products, pp. 807–812.

Haupt, W.A. (1981) Model tests on screening of surface waves, Proc. 10th Int. Conf. Soil Mech. Found. Eng., Stockholm, Vol. 3, pp. 215–222.

Hayakawa, K., Takeshita, S. and Matsui, T. (1991) Reduction effect of EPS blocks on ground vibration caused by road Traffic and its evaluation, Soils Found., Vol. 31, No. 2, pp. 226–234 (in Japanese).

Hayakawa, K., Takeshita, S. and Matsui, T. (1992) Ground vibration reduction due to vibration proof mats in railroad and its evaluation, Soils Found., Vol. 32, No. 1, pp. 249–259.

Massarsch, K.R. (1991) Ground vibration isolation using gas cushions, Proc. 2nd Int. Conf. Recent Adv. Geotech. Earthq. Eng. and Soil Dyn., St. Louis, Vol. II, pp. 1461–1470.

Massarsch, K.R. (2004) Mitigation of traffic-induced ground vibrations, Proc. 11th Int. Conf. Soil Dyn. Earthq. Eng. and the . Conf. Earthq. Geotech. Eng., Berkeley, Vol. 1, pp. 22–31.

Sannomiya, T., Towhata, I. and Kinugawa, H. (1993) Field tests on mitigation methods of ground vibration, Proc. Annual Conv. Japan. Soc. Soil Mech. Found. Eng., Vol. 1, Kobe, pp. 1261–1262 (in Japanese).

Takemiya, H. (2004) Field vibration mitigation by honeycomb WIB for pile foundations of a high-speed train viaduct, Soil Dyn. Earthq. Eng., Vol. 24, pp. 69–87.

Woods, R.D. (1968) Screening the surface waves in soils, Proc. ASCE, Vol.94, SM4, pp.951–979.